Enabling quantum non-Markovian dynamics by injection of classical colored noise

J. I. Costa-Filho,[1] R. B. B. Lima,[1] R. R. Paiva,[1] P. M. Soares,[1] W. A. M. Morgado,[2] R. Lo Franco,[3,4] and D. O. Soares-Pinto[1]

[1]*Instituto de Física de São Carlos, Universidade de São Paulo, CP 369, 13560-970, São Carlos, São Paulo, Brazil*

[2]*Department of Physics, PUC-Rio and National Institute of Science and Technology for Complex Systems, Rua Marquês de São Vicente 225, 22453-900, Rio de Janeiro-RJ, Brazil*

[3]*Dipartimento di Fisica e Chimica, Università di Palermo, via Archirafi 36, 90123 Palermo, Italy*

[4]*Dipartimento di Energia, Ingegneria dell'Informazione e Modelli Matematici, Università di Palermo, Viale delle Scienze, Edificio 9, 90128 Palermo, Italy*

(Received 27 January 2017; published 25 May 2017)

The non-Markovian nature of quantum systems recently turned to be a key subject for investigations on open quantum system dynamics. Many studies, from its theoretical grounding to its usefulness as a resource for quantum information processing and experimental demonstrations, have been reported in the literature. Typically, in these studies, a structured reservoir is required to make non-Markovian dynamics emerge. Here, we investigate the dynamics of a qubit interacting with a bosonic bath and under the injection of a classical stochastic colored noise. A canonical Lindblad-like master equation for the system is derived by using the stochastic wave function formalism. Then, the non-Markovianity of the evolution is witnessed by using the measure of Andersson, Cresser, Hall, and Li. We evaluate the measure for three different noises and study the interplay between environment and noise pump necessary to generate quantum non-Markovianity, as well as the energy balance of the system. Finally, we discuss the possibility to experimentally implement the proposed model.

DOI: 10.1103/PhysRevA.95.052126

I. INTRODUCTION

The unavoidable interaction of every quantum system with its surroundings is the central topic of study in the theory of open quantum systems [1–6]. One of its main objectives is to understand how the system loses information to the environment and how it could be recovered [7,8], which leads to the current interest in non-Markovian open quantum systems [9–15]. Non–Markovian environments display the desired memory effects and information backflows [9,16–19] but, in turn, usually need to be highly structured [20–28].

The concept of non-Markovianity, although well understood in classical stochastic processes [29], has no straightforward generalization to quantum systems. In classical probability theory, a stochastic process is Markovian if the conditional probability that it takes some value x_n at the time t_n, given it had the value x_{n-1} at time t_{n-1}, is independent of events prior to t_{n-1} [9,29]. In other words, the process is Markovian if the probability of going to some future state depends only on the present state and not on the previous ones, i.e., the process has no memory of its past states [9]. That definition does not work well in quantum mechanics, because we need to measure the system in its past states to formulate conditional probabilities. Since measurements in quantum mechanics disturb the system and, therefore, the conditional probabilities above, the definition of Markovianity would depend not only on the process to be analyzed but also on the choice of measurement scheme [9], which is a undesirable drawback.

To fix that, various definitions were proposed in the literature [1,2,4,18,30–32], but they are in most cases not equivalent to each other. On the one hand, the Rivas, Huelga, Plenio (RHP) definition [9] says that a quantum evolution is Markovian if it is CP-divisible, i.e., it satisfies a composition law analogous to the Chapman–Kolmogorov equation, which is obeyed by classical Markov processes [9,29]. On the other hand, the Breuer, Lane, Piilo (BLP) definition [33] states that, in Markovian processes, the distinguishability of quantum states subject to the same evolution does not increase over time, which is a way to state that the process is memoryless. Both definitions are not equivalent, as are many other definitions in the literature, which shows that quantum non-Markovianity is in reality a multifaceted phenomenon.

As broad as the different definitions of quantum non-Markovianity is the plethora of its features and applications. Quantum non-Markovianity is related, for example, to preservation of coherence [34], energy backflows [35], speedup of quantum speed limits [36], violations of the Landauer bound [37], formation of steady-state entanglement [38], revivals and protection of entanglement [39–45], and is an obstacle to quantum Darwinism [46]. It has applications from quantum metrology [21], superdense coding [47], and quantum cryptography [48] to quantum control [49]. Recently, many experiments were conducted that verify or take advantage of non-Markovian features [50–55]. Finally, non-Markovianity is necessary for a realistic description of some quantum systems, such as strongly coupled systems [56,57], some spin baths [58], biological systems [59], complex nanostructures [60], and photosynthetic systems [61]. As can be seen, quantum non-Markovianity is an invaluable resource for quantum technologies, which needs to be completely understood and harnessed.

In this paper, we show that one alternative to reservoir engineering is to induce quantum non-Markovianity by injection of classical noise [62–69]. A sufficiently strong noise could reverse the information flow from the system to the environment, thereby leading to memory effects. The procedure is as follows: We use the stochastic wave function's formalism [70,71], where the state of the system is described by an ensemble of pure states, and the system density matrix is recovered by an averaging process. The environment is a thermal bath in the Born–Markov setting [1,2], while the classical noise is modeled by a stochastic Hamiltonian

 ©2017 American Physical Society

[62–64]. Finally, the master equation of the system is derived using functional techniques [72–74], and a non-Markovianity measure [75] is used to show that the evolution is indeed non-Markovian. We specifically use the Andersson, Cresser, Hall, and Li (ACHL) [75] measure, since it can be applied directly to the master equation of the system. The definitions of quantum non-Markovianity are in general nonequivalent, and so are its measures, thus we also relate the ACHL measure to other known measures of non-Markovianity.

The structure of the paper is arranged as follows: In Sec. II we review the definition of quantum non-Markovianity, the ACHL non-Markovianity measure and its relation to other measures, while in Sec. III the master equation of the problem is derived. The results are discussed in Sec. IV, where different noises are applied to the master equation and its non-Markovianity is measured. An experimental proposal is made in Sec. V and, finally, Sec. VI contains the conclusion.

II. QUANTUM NON-MARKOVIANITY

A. Definition

In this paper we consider two quantum non-Markovianity definitions: the RHP [2] and BLP conditions [33]. The RHP condition states that a quantum process $\mathcal{E}(t,t_0)$ is Markovian if it is a CP-divisible map, i.e., a trace-preserving, completely positive (CPTP) map such that, for any intermediate time, it can be broken into two CPTP maps; namely,

$$\mathcal{E}(t,t_0) = \mathcal{E}(t,t_1)\mathcal{E}(t_1,t_0), \quad t_0 \leqslant t_1 \leqslant t, \tag{1}$$

where $\mathcal{E}(t,t_1)$ and $\mathcal{E}(t_1,t_0)$ are CPTP maps. The BLP defines Markovianity as an evolution such that the trace distance between any two states decreases monotonically with time:

$$\frac{d}{dt}||\rho_1(t) - \rho_2(t)||_1 \leqslant 0, \tag{2}$$

where $\rho(t) = \mathcal{E}(t,t_0)[\rho]$ and $||X||_1 = \mathrm{tr}\sqrt{XX^\dagger}$. Physically, it means that, in a Markovian evolution, the indistinguishability between any two states cannot increase. We should stress a difference between the classical and quantum cases: the well-defined classical trajectories, that diverge for systems with positive Lyapunov exponents do obey Markovian equations of motion. To understand how the two definitions of Markovianity are related to each other, we need the concept of k-divisibility.

A quantum evolution $\mathcal{E}$ is positive if it takes positive operators (such as density operators) to positive operators, and is k-positive if $\mathbb{1}_k \otimes \mathcal{E}$ is a positive evolution. If the evolution is k-positive for every $k \in \mathbb{N}$ less than or equal to the dimension of the system, then it is completely positive (CP). These concepts can be generalized to continuous in time evolutions: a k-divisible map [76] is a k-positive map which can be arbitrarily broken into two other k-positive maps, and a CP-divisible map is simply a map which is k-divisible for every $k \in \mathbb{N}$. For simplicity, we call 1-divisible maps as P-divisible maps. Now we are able to link the two definitions: the BLP and RHP conditions are equivalent to the map being P-divisible and CP-divisible, respectively, as shown in Ref. [76]. Therefore, every non-Markovian evolution in the BLP sense is non-Markovian in the RHP sense, but not the converse.

B. Decay-rate measure

The most general form of a completely positive, trace-preserving Markovian (in the RHP sense) master equation is given by Lindblad's theorem [4,77]:

$$\begin{aligned}\frac{d\rho(t)}{dt} &= \mathcal{L}_t[\rho(t)] = -i[H(t),\rho(t)] \\ &\quad + \sum_{\alpha,\beta}\gamma_{\alpha\beta}(t)\left[A_\beta(t)\rho(t)A_\alpha^\dagger(t) - \frac{1}{2}\{A_\alpha^\dagger(t)A_\beta(t),\rho(t)\}\right],\end{aligned} \tag{3}$$

where the $A_\alpha(t)$ are general operators acting on the system, $H(t)$ is a Hermitian operator, and $\gamma_{\alpha\beta}(t) \geqslant 0$, for every α, β, and t. However, master equations obeying the form of Eq. (3) and with possibly negative decay (or decoherence) rates $\gamma_{\alpha\beta}(t)$ can represent more general time-local master equations [75], such as non-Markovian ones. With that in mind, the negativity of the decay rates can be used as a measure of non-Markovianity and is a very suitable measure since it applies directly to the master equation.

The above measure, however, faces a problem: the Lindblad form is nonunique, and the same set of coefficients $\gamma_{\alpha\beta}(t)$ may generate different dynamics. To circumvent that issue, the canonical form [9,75] of Lindblad-like equations is used. This form is obtained by expressing the Lindbladian in a orthonormal operator space basis, i.e., a basis $\{G_k\}_0^{d^2-1}$ such that $\mathrm{tr}[G_i^\dagger G_j] = \delta_{ij}$, where d is the dimension of the Hilbert space and, for simplicity, $G_0 = \mathbb{1}/\sqrt{d}$ [2]. In that basis,

$$A_\beta(t) = \sum_n a_{\beta n}(t)G_n, \quad a_{\beta n}(t) = \mathrm{tr}[G_n^\dagger V_\beta(t)], \tag{4}$$

$$A_\alpha^\dagger(t) = \sum_m a_{\alpha m}^*(t)G_m^\dagger, \quad a_{\alpha m}^*(t) = \mathrm{tr}[G_m V_\alpha^\dagger(t)], \tag{5}$$

where the operators V_α shall be associated with the stochastic noise in the following. The master equation is

$$\begin{aligned}\frac{d\rho(t)}{dt} &= -i[H(t),\rho(t)] \\ &\quad + \sum_{n,m}c_{nm}(t)\left[G_n\rho(t)G_m^\dagger - \frac{1}{2}\{G_m^\dagger G_n,\rho(t)\}\right],\end{aligned} \tag{6}$$

where $c_{nm} = \sum_{\alpha,\beta} a_{\alpha m}^*(t)\gamma_{\alpha\beta}(t)a_{\beta n}(t)$. It is straightforward to show that the c_{nm} form a Hermitian matrix C just by using the fact that the $\gamma_{\alpha\beta}(t)$ also form a Hermitian matrix. Since every Hermitian matrix can be diagonalized by a unitary operation, $C = UDU^\dagger$, with U and D being unitary and diagonal matrices, respectively, we have that the coefficients of C are given by $c_{nm} = \sum_k u_{nk}(t)\gamma_k(t)u_{mk}^*(t)$, where $u_{nk}(t)$ are coefficients of the unitary matrix U. Equation (6) is now written as

$$\begin{aligned}\frac{d\rho(t)}{dt} &= -i[H(t),\rho(t)] + \sum_k \gamma_k(t) \\ &\quad \times \left[L_k(t)\rho(t)L_k^\dagger(t) - \frac{1}{2}\{L_k^\dagger(t)L_k(t),\rho(t)\}\right],\end{aligned} \tag{7}$$

where

$$L_k(t) = \sum_n u_{nk}(t) G_n, \tag{8}$$

$$L_k^\dagger(t) = \sum_m u_{mk}^*(t) G_m, \tag{9}$$

still form an orthonormal basis, since unitary operations preserve inner products.

The $\gamma_k(t)$ are the canonical decay rates and with them we can build the measures of non-Markovianity. Define [75]

$$f(t) = \sum_{k=1}^{d^2-1} \max\{-\gamma_k(t), 0\} = \frac{1}{2} \sum_{k=1}^{d^2-1} [|\gamma_k(t)| - \gamma_k(t)]. \tag{10}$$

The decay rates or ACHL measure [75] for the time interval $t_0 \leqslant \tau \leqslant t$ is

$$\mathcal{N}_{\text{ACHL}} = \int_{t_0}^{t} f(\tau) d\tau. \tag{11}$$

Note that $\max\{-\gamma_k(t), 0\}$ simply selects the negative part of each $\gamma_k(t)$ and is zero if it is strictly nonnegative. The term $f(t)$ sums the contributions of all negative decay rates, and $\mathcal{N}_{\text{ACHL}}$ is this contribution integrated along the time interval.

The ACHL measure is nonzero if at least one decay rate is negative, for any brief interval of time, since this is sufficient for the breakdown of CP-divisibility [9]. That condition, however, for most cases is not sufficient to break P-divisibility. Therefore, some BLP Markovian evolutions can be considered non-Markovian by this measure.

C. Relation with other measures

The decay-rate measure can be related to other non-Markovianity measures. The RHP measure [16] estimates the breakdown of CP-divisibility by computing how the intermediate dynamics deviates from complete positivity. Namely, given a quantum evolution $\mathcal{E}(t, t_0)$, it can be decomposed as in Eq. (1), since the map is continuous in time. Supposing that, for some t_1, $\mathcal{E}^{-1}(t_1, t_0)$ exists, then the intermediate dynamical map

$$\mathcal{E}(t, t_1) = \mathcal{E}(t, t_0) \mathcal{E}^{-1}(t_1, t_0), \tag{12}$$

is well defined. An evolution is non-Markovian if there exists at least an intermediate time t_1 such that $\mathcal{E}(t, t_1)$ is not completely positive, and the latter is completely positive if its Choi matrix [78,79]

$$J(\mathcal{E}(t, t_1)) = \frac{1}{d} \sum_{i,j=1}^{d} |i\rangle \langle j| \otimes \mathcal{E}(t, t_1)[|i\rangle \langle j|], \tag{13}$$

where $|i\rangle$ is an orthonormal basis for the system, is positive semidefinite. Since our evolution is trace preserving, Eq. (13) is positive definite if its 1-norm is equal to unity [9]. With that in mind, we define

$$g(t) = \lim_{\epsilon \to 0^+} \frac{||J(\mathcal{E}(t+\epsilon, t))||_1 - 1}{\epsilon}, \tag{14}$$

and $g(t) > 0$ if and only if the evolution is non-Markovian. Then, the RHP measure is

$$\mathcal{N}_{\text{RHP}} = \int_{t_0}^{t} g(\tau) d\tau. \tag{15}$$

The RHP measure is proportional to the ACHL measure [9,16,75]:

$$\mathcal{N}_{\text{ACHL}} = \frac{d}{2} \mathcal{N}_{\text{RHP}}. \tag{16}$$

An interesting case is the qubit, where both measures are equivalent.

Another common measure is the BLP measure [33], related to the BLP condition, and which measures the increase of distinguishability of quantum states. For any two states $\rho_1(t)$ and $\rho_2(t)$ undergoing the same evolution, their trace distance

$$D(\rho_1(t), \rho_2(t)) = \tfrac{1}{2} \mid \rho_1(t) - \rho_2(t) \mid, \tag{17}$$

is nonincreasing under completely positive evolutions [1,80],

$$\sigma(t, \rho_1, \rho_2) = \frac{d}{dt} D(\rho_1(t), \rho_2(t)) < 0. \tag{18}$$

The BLP measure is defined as

$$\mathcal{N}_{\text{BLP}} = \max_{\rho_1, \rho_2} \int_{\sigma > 0} \sigma\left(t', \rho_1, \rho_2\right) dt', \tag{19}$$

where the integral is evaluated over time intervals on which $\sigma > 0$. The measure is the maximum distance for two states for any possible initial states ρ_1 and ρ_2. Although its computation is nontrivial, its relationship with the decay rates measure can be studied for the case of a single qubit [75].

Since qubits can be represented in Bloch form [80],

$$\rho = \tfrac{1}{2}(\mathbb{1} + \vec{n} \cdot \vec{\sigma}), \tag{20}$$

where $\vec{n}$ is its Bloch vector, any master equation in Lindblad form,

$$\frac{d\rho(t)}{dt} = \mathcal{L}_t[\rho(t)], \tag{21}$$

can be rewritten in terms of the Bloch vector as

$$\dot{\vec{n}} = D(t)\vec{n} + \vec{u}(t), \tag{22}$$

where

$$D_{jk}(t) = \tfrac{1}{2} \text{tr}[\sigma_j^\dagger \mathcal{L}_t(\sigma_k)], \tag{23}$$

$$u_j(t) = \tfrac{1}{2} \text{tr}[\sigma_j^\dagger \mathcal{L}_t(\mathbb{1})], \tag{24}$$

are the matrix elements of the so-called damping matrix $D(t)$ and the drift vector $\vec{u}(t)$, respectively [75].

The increase of trace distance between two arbitrary qubits is only possible if the increase occurs at infinitesimal distance. For any two infinitesimally separated qubits ρ and $\rho + \delta\rho$, their squared trace distance is [75]

$$D^2(\rho, \rho + \delta\rho) = \tfrac{1}{4} \delta\vec{n} \cdot \delta\vec{n}, \tag{25}$$

and it can be shown that it increases if the matrix $(D + D^T)(t)$ has a positive eigenvalue [75]. For a qubit under amplitude

damping [1,2], the case which will be studied in this article, this condition boils down to

$$\sum_{k=1}^{2}\gamma_k(t) < 0, \tag{26}$$

and a related measure is

$$h(t) = \max\left\{-\sum_{k=1}^{2}\gamma_k(t), 0\right\}, \tag{27}$$

$$\mathcal{N}_{\mathrm{BLP}} = \int_{t_0}^{t} h(\tau)d\tau. \tag{28}$$

This condition is stronger than the required in the ACHL measure in Eq. (10), since it needs the sum of all decay rates to be negative, and not just one of them. Then, for example, we could have Markovianity even in the presence of a negative decay rate, given the other decay rates were large enough to make the sum in Eq. (27) positive. As a consequence, for single decoherence channels both measures are equivalent.

The Bloch volume measure [81], whose application is restricted to qubits, is another non-Markovianity measure. Since the volume, in the Bloch sphere, of accessible states under a CP quantum evolution only decreases, its increase can be related to non-Markovianity [9,81]. Using the damping matrix, it is possible to show [75] that non-Markovianity emerges if and only if Eq. (26) holds, so there is an equivalence between the Bloch volume and BLP measures. Note that these measures are inequivalent in more general scenarios [9,75].

In the next section we deduce the canonical master equation of a qubit in a bosonic bath and under the influence of a classical colored noise. After that, it is possible to use the ACHL measure and study the non-Markovian character (in the RHP sense) of the evolution.

III. STOCHASTIC PUMPING AND AMPLITUDE DAMPING

A. System-environment evolution

Our first step is deriving a master equation in Lindblad form for a system interacting with a bath. Let us consider an evolution described by the Hamiltonian

$$H = \frac{\omega_0}{2}\sigma_z + \sum_r \omega_r b_r^\dagger b_r + \sum_r g_r\left(\sigma_- b_r^\dagger + \sigma_+ b_r\right), \tag{29}$$

which describes a two-level system coupled to a bosonic bath [2], and where ω_0 is the system frequency, $b_r^\dagger$ (b_r) is the creation (annihilation) operator of the environment, and g_k is a coupling constant. The third term on the right-hand side of Eq. (29) is the Hamiltonian H_{int}, responsible for the system-bath interaction, which can be written as

$$\begin{aligned} H_{\mathrm{int}} &= \sigma_- \otimes \sum_r g_r b_r^\dagger + \sigma_+ \otimes \sum_r g_r b_r \\ &\equiv A_1 \otimes B_1 + A_2 \otimes B_2. \end{aligned} \tag{30}$$

The Liouville-von Neumann equation [82] for the Hamiltonian in Eq. (29), in the interaction picture, is

$$\frac{d}{dt}\tilde{\rho}(t) = -i[\tilde{H}_{\mathrm{int}}(t), \tilde{\rho}(t)], \tag{31}$$

where $\tilde{A}$ means that the corresponding operator is in the interaction picture, and

$$\begin{aligned} \tilde{H}_{\mathrm{int}}(t) &= e^{-i\omega_0 t}\sigma_- \otimes \sum_r g_r e^{-i\omega_r t} b_r^\dagger + e^{-i\omega_0 t}\sigma_+ \otimes \sum_r g_r e^{i\omega_r t} b_r \\ &\equiv \tilde{A}_1(t) \otimes \tilde{B}_1(t) + \tilde{A}_2(t) \otimes \tilde{B}_2(t). \end{aligned} \tag{32}$$

To obtain the system's evolution, we must trace over the bath's degree of freedom [77] and resort to the Born–Markov approximation [1,2]. Namely, we assume that the reservoir correlation functions (RCFs) decay rapidly compared with the system evolution, so that we can work in a timescale where they are negligible and, therefore, memory effects are absent. The RCFs are

$$\mathcal{B}_{\alpha\beta}(t) = \mathrm{tr}_B[\tilde{B}_\alpha(t) B_\beta \rho_B], \tag{33}$$

where α, β are the indexes related to the interaction term H_{int} and, in the case of Eq. (32), range from 1 to 2. The approximation is valid if we work in the weak-coupling limit, i.e., we assume that the coupling constant g_k is small, and the initial state is uncorrelated,

$$\rho(0) = \rho_S(0) \otimes \rho_B, \tag{34}$$

where ρ_S is the system density operator and $\rho_B = \exp(-\beta H_S)/Z$, with $Z = \mathrm{tr}[\exp(-\beta H_S)]$ and $\beta = 1/T$, the environment density operator is in a thermal state. The RCFs of our problem are

$$\mathcal{B}_{11}(t) = \sum_r |g_r|^2 e^{i\omega_r t} N(\omega_r), \tag{35}$$

$$\mathcal{B}_{22}(t) = \sum_r |g_r|^2 e^{-i\omega_r t}[1 + N(\omega_r)], \tag{36}$$

where $N(\omega_r) = 1/[\exp(\omega_r/T) - 1]$ is the density of states in the mode ω_r [1], and the other RCFs $\mathcal{B}_{12}(t)$ and $\mathcal{B}_{21}(t)$ are zero. After performing the continuum limit,

$$\sum_r f(\omega_r) \to \int_0^\infty d\omega \frac{J(\omega)}{|g(\omega)|^2} f(\omega), \tag{37}$$

where $J(\omega)$ is the spectral density of the bath and $f(\omega_k)$ is an arbitrary function of the bath frequencies, the (nonzero) RCFs become

$$\mathcal{B}_{11}(\tau) = \int_0^\infty d\omega J(\omega) e^{i\omega\tau} N(\omega), \tag{38}$$

$$\mathcal{B}_{22}(\tau) = \int_0^\infty d\omega J(\omega) e^{-i\omega\tau}[1 + N(\omega)]. \tag{39}$$

The decay rates are Fourier transforms of the RCFs, and the final master equation for the system, in the Schrödinger picture where $\rho_S = \mathrm{tr}_B(\rho)$, is [2]

$$\begin{aligned} &\frac{d}{dt}\rho_S(t) \\ &= -i\left[\frac{\omega_0}{2}\sigma_z + H_{\mathrm{LS}}, \rho_S(t)\right] \\ &\quad + \gamma(\omega_0)N(\omega_0)\left[\sigma_+\rho_S(t)\sigma_- - \frac{1}{2}\{\sigma_-\sigma_+, \rho_S(t)\}\right] \\ &\quad + \gamma(\omega_0)[1 + N(\omega_0)]\left[\sigma_-\rho_S(t)\sigma_+ - \frac{1}{2}\{\sigma_+\sigma_-, \rho_S(t)\}\right], \end{aligned} \tag{40}$$

where $\gamma(\omega_0) = 2\pi J(\omega_0)$ and $H_{\rm LS}$ is the Lamb-shift Hamiltonian [2,83],

$$H_{\rm LS} = \left(\mathcal{P}\int_0^\infty d\omega \frac{J(\omega)[N(\omega)+1/2]}{\omega_0-\omega}\right)\sigma_z, \tag{41}$$

where $\mathcal{P}$ represents the Cauchy principal value. The term $H_{\rm LS}$ is simply a shift in the energy levels of the system.

B. System-noise evolution

The next step is to study the evolution of a quantum system under the influence of stochastic pumping of classical fields [64,65]. In this model, the Liouville-von Neumann equation of the system is given by

$$\frac{d}{dt}\rho(t) = -i\left[\frac{\omega_0}{2}\sigma_z + V(t),\rho(t)\right]. \tag{42}$$

The term $V(t)$, responsible for the classical noise, is

$$\begin{aligned} V(t) &= i[e^{-i\omega t}u(t)\sigma_- - e^{i\omega t}u^*(t)\sigma_+] \\ &\equiv \xi_1(t)V_1 + \xi_2(t)V_2, \end{aligned} \tag{43}$$

where $\xi(t)$ is a stochastic variable. We assume that it is a colored Gaussian noise with zero mean [29],

$$\overline{\xi(t)} = 0, \tag{44}$$

$$\overline{\xi(t)\xi(t')} = \overline{\xi^*(t)\xi^*(t')} = 0, \tag{45}$$

$$\overline{\xi^*(t)\xi(t')} = \overline{\xi(t)\xi^*(t')} \equiv \chi(t,t'), \tag{46}$$

where the bar denotes an average over the stochastic realizations [64].

To deal with this stochastic behavior we use the stochastic wave-function formalism [3] in which the state of an open quantum system is described by an ensemble of pure states $\rho(t) = |\Psi(t)\rangle\langle\Psi(t)|$ [64]. The density matrix of the system is recovered after an average over the stochastic realizations [29]

$$\rho_S(t) = \overline{\rho(t)}. \tag{47}$$

Taking the average over Eq. (42), we have that

$$\frac{d}{dt}\rho_S(t) = i\left[\frac{\omega_0}{2}\sigma_z,\rho(t)\right] - i[\overline{V(t)\rho(t)} - \overline{\rho(t)V(t)}]. \tag{48}$$

To calculate the terms $\overline{V(t)\rho(t)}$ and $\overline{\rho(t)V(t)}$ we apply Novikov's theorem [72,73],

$$\overline{\xi(t)\rho[\xi]} = \int_0^t dt'\overline{\xi(t)\xi(t')}\overline{\frac{\delta\rho[\xi]}{\delta\xi(t')}}, \tag{49}$$

which considers the average of the product of a stochastic process $\xi(t)$ and its functional form $\rho[\xi]$, and where the last term on the right-hand side is a functional derivative [73]. Following the steps of Refs. [64,65] and assuming a weak coupling between system and pumping [62], Eq. (48) takes the form

$$\begin{aligned} \frac{d}{dt}\rho_S(t) =& -i\left[\frac{\omega_0}{2}\sigma_z,\rho_S(t)\right] \\ &- \sum_{\alpha,\beta}\int_0^t dt'\chi_{\alpha\beta}(t,t')[V_\alpha^\dagger(t),[V_\beta(t'),\rho_S(t)]]. \end{aligned} \tag{50}$$

Evaluating Eq. (50) and assuming homogeneity in time correlations, i.e., $\chi_{\alpha\beta}(t,t') = \chi_{\alpha\beta}(t-t') \equiv \mathcal{S}(\tau)$, the master equation, in Lindblad form, is

$$\begin{aligned} \frac{d}{dt}\rho_S(t) =& -i\left[\frac{\omega_0}{2}\sigma_z + H_{\rm EFF}(t),\rho_S(t)\right] \\ &+ \eta(t)\left[\sigma_+\rho_S(t)\sigma_- - \frac{1}{2}\{\sigma_-\sigma_+,\rho_S(t)\}\right] \\ &+ \eta(t)\left[\sigma_-\rho_S(t)\sigma_+ - \frac{1}{2}\{\sigma_+\sigma_-,\rho_S(t)\}\right], \end{aligned} \tag{51}$$

where

$$\eta(t) = 2\int_0^t d\tau\mathcal{S}(\tau)\cos(\Delta\omega\tau), \tag{52}$$

and $H_{\rm EFF}(t)$ appears due the coupling between the system and the stochastic pumping and represents a shift in the system energy levels. It is defined as

$$H_{\rm EFF}(t) = \int_0^t d\tau\mathcal{S}(\tau)\sin(\Delta\omega\tau)\sigma_z, \tag{53}$$

and $\Delta\omega = \omega - \omega_0$. An analogous derivation, but using white Gaussian noise, is presented in Ref. [84].

C. Combined evolution

Combining the evolutions of Eqs. (40) and (51), the complete master equation for the system takes the form

$$\begin{aligned} \frac{d}{dt}\rho(t) =& -i\left[\frac{\omega_0}{2}\sigma_z + H_{\rm shift}(t),\rho(t)\right] \\ &+ \gamma_1(t)\left[\sigma_+\rho(t)\sigma_- - \frac{1}{2}\{\sigma_-\sigma_+,\rho(t)\}\right] \\ &+ \gamma_2(t)\left[\sigma_-\rho(t)\sigma_+ - \frac{1}{2}\{\sigma_+\sigma_-,\rho(t)\}\right], \end{aligned} \tag{54}$$

where the coefficients of the master equation,

$$\gamma_1(t) = \gamma N(\omega_0) + \eta(t), \tag{55}$$

$$\gamma_2(t) = \gamma[1+N(\omega_0)] + \eta(t), \tag{56}$$

are the decay rates. The term $H_{\rm shift}(t)$ is the sum of the energy shifts $H_{\rm LS}$ and $H_{\rm EFF}(t)$. Note that the master equation is already in canonical form, so the ACHL measure can be applied directly to its decay rates.

The decay rates in Eqs. (55) and (56) are composed of two terms: one related to the bath and the other to the noise pump. The first is always positive, and the second, which is time dependent, can be either positive or negative. Therefore, the non-Markovian character of the evolution, determined by the negativity of the decay rates [75], depends on the relative strength between system-bath and system-pump interactions.

The evolution is RHP Markovian when the temperature terms are greater, in absolute value, than the negative part of $\eta(t)$. Then, a question can be asked: which is the minimum temperature above which the evolution is RHP Markovian or, equivalently, the maximum temperature under which the evolution shows RHP non-Markovian effects? Following the ACHL criterion given in Eqs. (10) and (11), it is determined by the point where at least one of the decay rates becomes negative. Since $\gamma_1(t)$ is always smaller than $\gamma_2(t)$, that point is when $\gamma N(\omega_0) + \eta_{\min} = 0$, where

$$\eta_{\min} = \min_{t_0 \leqslant \tau \leqslant t} \eta(\tau). \tag{57}$$

Then, a RHP Markovianity temperature can be set as

$$T := \frac{\omega_0}{\ln\left(1 - \frac{\gamma}{\eta_{\min}}\right)}. \tag{58}$$

This is the temperature below which RHP non-Markovian features emerge.

The master equation for the qubit population $\rho_{11}(t)$ takes the simple form

$$\frac{d}{dt}\rho_{11}(t) = -[\gamma_1(t) + \gamma_2(t)]\rho_{11}(t) + \gamma_1(t), \tag{59}$$

and the other population is constrained by the unitarity of the trace of the density operator: $\rho_{22}(t) = 1 - \rho_{11}(t)$. It is simpler, however, to put the qubit density matrix in Bloch form, Eq. (20), and study the evolution of the z component of the Bloch vector, $n_z(t) = \langle \sigma_z(t) \rangle$:

$$\frac{d}{dt}n_z(t) = -[\gamma_1(t) + \gamma_2(t)]n_z(t) + \gamma_1(t) - \gamma_2(t). \tag{60}$$

In terms of $n_z(t)$, the average energy of the system is

$$\langle E \rangle = \mathrm{tr}\left[\frac{\omega_0}{2}\sigma_z \rho(t)\right] = \frac{\omega_0}{2} n_z(t). \tag{61}$$

For long times, $t \to \infty$, the system thermalizes and the rate of change of $n_z(t)$ is zero. Therefore, the average energy tends to the value

$$\langle E \rangle = -\frac{\omega_0}{2}\left[\frac{1}{2N(\omega_0) + 1 + 2\eta_\infty/\gamma}\right], \tag{62}$$

where η_∞ is the limit of $\eta(t)$ as $t \to \infty$. Without the noise, the average energy converges to the value

$$\langle E_{\text{no pump}} \rangle = -\frac{\omega_0}{2}\left[\frac{1}{2N(\omega_0) + 1}\right], \tag{63}$$

and therefore the energy difference $\langle E \rangle - \langle E_{\text{no pump}} \rangle$ is

$$\Delta E = \frac{\omega_0}{2}\frac{\gamma}{2\eta_\infty}\left[1 + \left(\frac{2\eta_\infty}{\gamma(2N(\omega_0) + 1)}\right)\right]^{-1}. \tag{64}$$

Note that, since η_∞ is usually very small, if we vary $N(\omega_0)$ the energy difference will not change considerably.

IV. ROLE OF STOCHASTIC NOISE

A. Exponential noise

In this section we study Eq. (54) for different classical stochastic noise injections, which are defined by their correlation functions $\mathcal{S}(\tau)$. The first noise correlation which we analyze is an exponential decay [67] (which characterizes the Ornstein–Uhlenbeck process),

$$\mathcal{S}_{\text{OU}}(\tau) = \frac{\Omega}{2\tau_c} e^{-\tau/\tau_c}, \tag{65}$$

where Ω is an amplitude and τ_c is the correlation time. The Ω must remain small, since otherwise the weak-coupling assumption would be violated. The exact formula for $\eta(t)$ is

$$\eta(t) = \frac{\Omega}{1 + (\Delta\omega\tau_c)^2} \times [1 + \sqrt{1 + (\Delta\omega\tau_c)^2}\, e^{-t/\tau_c} \sin(\Delta\omega t - \phi)], \tag{66}$$

where

$$\phi = \sin^{-1}\left[\frac{1}{\sqrt{1 + (\Delta\omega\tau_c)^2}}\right]. \tag{67}$$

Note that the function $\eta(t)$ is composed of a constant term and a damped oscillating term.

We will consider a system where $T = c\omega_0$ wherein c is a constant, i.e., we define the temperature as a function of the frequency of the system. Fixing all other parameters but the product $\Delta\omega\tau_c$, $\eta(t)$ reaches a global minimum value when $\Delta\omega\tau_c = 8.5$. With these conditions, the only remaining free parameter is Ω. Now, we want to find the Markovian to non-Markovian transition, i.e., the smallest value of Ω for which the decay rates have a negative part. Physically, we are looking for the smallest pump intensity for which the system reaches the RHP Markovianity limit, where this limit identifies the border between the two regimes. That value is $\Omega = 0.91$, which corresponds to the situation when the decay rate $\gamma_1(t)$ touches the horizontal axis. The coefficients $\eta(t)$ and $\gamma_1(t)$ are plotted in Fig. 1.

If we assume that the initial state of the system is $\rho(0) = |+\rangle\langle+|$, and $|+\rangle = \frac{1}{\sqrt{2}}(|0\rangle + |1\rangle)$ [which implies that $n_z(0) = 0$], then the average energy of the system can be calculated. The average energy with (E_P) and without (E_{NP}) pump, as well as the difference ($\Delta E = E_P - E_{NP}$), at $T = 0.1\omega_0$, are shown in Fig. 2(a), in units of ω_0. Note that the average energy tends to a bigger value when the pump acts on the system, than when it is absent.

Note that, for short times, i.e., $t \ll \tau_c$, we have

$$\eta_{\text{OU}}(t) \simeq \frac{\Omega t}{\tau_c}. \tag{68}$$

For the opposite limit, $t \to \infty$,

$$\eta_{\text{OU}} \to \frac{\Omega}{1 + (\Delta\omega\tau_c)^2}, \tag{69}$$

and the average energy tends to

$$\langle E \rangle \to -\frac{\omega_0}{2}\left[\frac{1}{2N(\omega_0) + 1 + \frac{2\Omega}{1 + (\Delta\omega\tau_c)^2}}\right]. \tag{70}$$

Now the temperature is lowered to $T = 0.1\omega_0$, where RHP non-Markovian effects are present. The average energy is plotted in Fig. 2(b), and the decay rate $\gamma_1(t)$ and the ACHL measure $f(t)$ are plotted in Fig. 3. We can see that the average energy increases compared with the Markovian case, due to its dependence with the density of the states, $\langle E \rangle \propto 1/N(\omega_0)$.

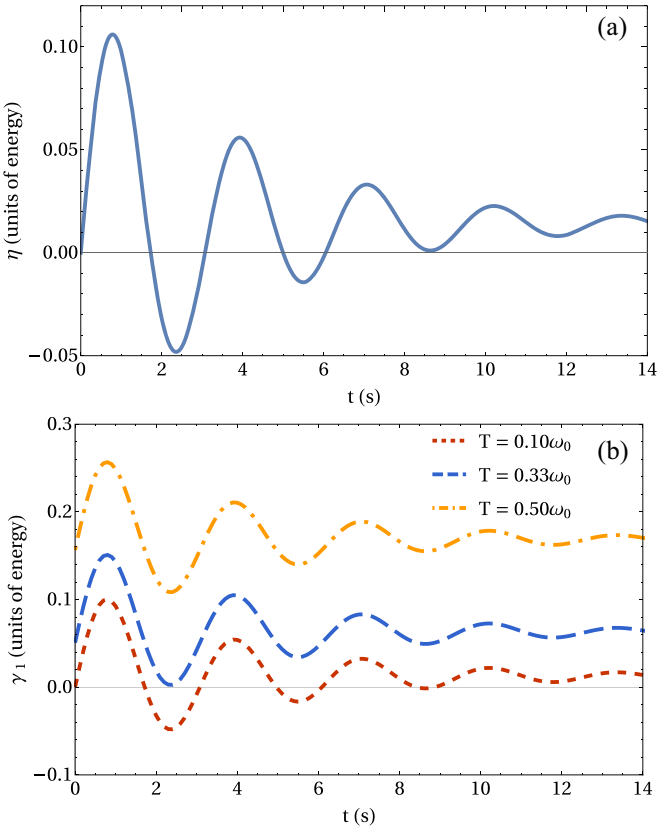

FIG. 1. (a) $\eta(t)$, defined in Eq. (52), and (b) $\gamma_1(t)$, defined in Eq. (55), as a function of time using the exponential pump for three different temperatures: $T = 0.10\omega_0$ (short-dashed red line), $T = 0.33\omega_0$ (long-dashed blue line), which characterizes the limit to find RHP Markovian dynamics in the system and $T = 0.50\omega_0$ (dot-dashed yellow line). Note that the condition to achieve RHP non-Markovianity is $\eta_{\min} < 0$. For all the curves used, $\Delta\omega = 2$, $\tau_c = 4.25$, $\Omega = 0.91$, $\gamma = 1$.

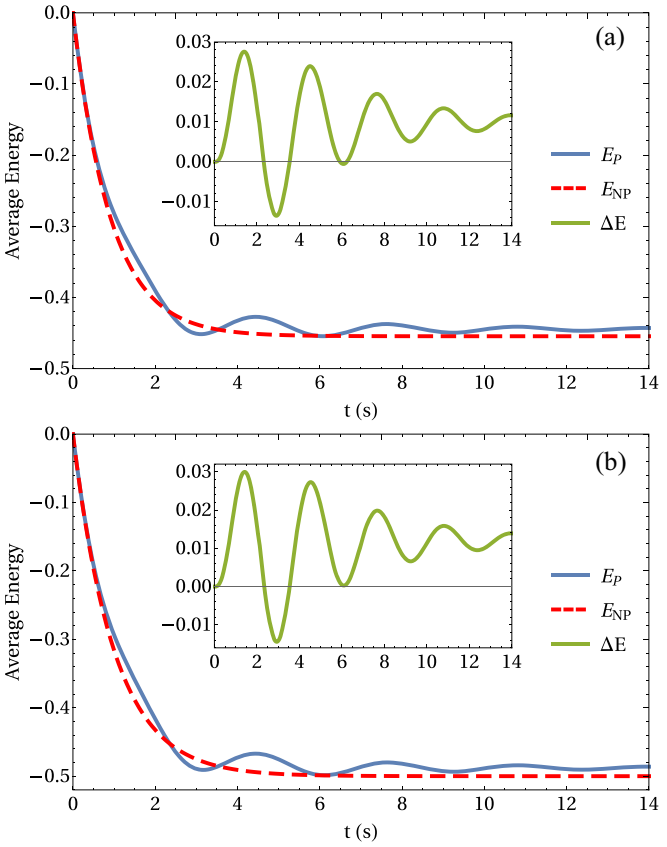

FIG. 2. Average energy of the system, in units of ω_0, with (E_P, blue solid line) and without (E_{NP}, red dashed line) exponential pump. Inset shows average energy difference, defined as $\Delta E = E_P - E_{NP}$. (a) RHP Markovian regime, with $T = 0.33\omega_0$, and (b) RHP non-Markovian regime, with $T = 0.10\omega_0$. The parameters used were $\Delta\omega = 2$, $\tau_c = 4.25$, $\Omega = 0.91$, $\gamma = 1$. We can observe that the energy differences in the two regimes are equivalent; thus, the energy cost to generate RHP non-Markovianity is low.

The energy difference, however, remains small, which suggests that, in this scheme, we can induce RHP non-Markovianity without too much energy cost. For the decay rate $\gamma_1(t)$, negative regions can be observed, which is a sign of non-Markovianity. These regions generate the peaks in the ACHL measure. The values obtained for the measure were $\mathcal{N}_{\text{ACHL}} = 0.0546$ for $T = 0.1\omega_0$ and $\mathcal{N}_{\text{ACHL}} = 0.0046$ for $T = 0.3\omega_0$.

B. Squared exponential noise

The squared exponential correlation function is [67]

$$\mathcal{S}_{\text{SE}}(\tau) = \frac{\Omega}{\sqrt{\pi}\tau_c} e^{-(t/\tau_c)^2}, \tag{71}$$

and for the same parameters as in the exponential case, we reach the RHP Markovian limit with $\Omega = 0.47$. The average energies for $T = 0.33\omega_0$ and $T = 0.10\omega_0$ are plotted in Fig. 4. Note that, for this noise, the difference in the energies is almost negligible. For short times,

$$\eta_{\text{SE}}(t) \simeq \frac{2\Omega t}{\sqrt{\pi}\tau_c}, \tag{72}$$

and for the long-time limit,

$$\eta_{\text{SE}} \to \Omega e^{-(\Delta\omega\tau_c/2)^2}. \tag{73}$$

The average energy tends to

$$\langle E\rangle \to -\frac{\omega_0}{2}\left[\frac{1}{2N(\omega_0)+1+2\Omega e^{-(\Delta\omega\tau_c/2)^2}}\right]. \tag{74}$$

The decay rate $\gamma_1(t)$ and the ACHL measure $f(t)$ are plotted in Fig. 5. In this case, the values for the measure were $\mathcal{N}_{\text{ACHL}} = 0.0585$ for $T = 0.10\omega_0$ and $\mathcal{N}_{\text{ACHL}} = 0.0040$ for $T = 0.30\omega_0$.

C. Power-law noise

For the power-law noise [67],

$$\mathcal{S}_{\text{PL}}(\tau) = \frac{(\alpha-1)}{2}\frac{\Omega}{\tau_c}\frac{1}{(\tau/\tau_c+1)^{\alpha}}, \tag{75}$$

where $\alpha > 2$, we have a global minimum (using $\alpha = 3$) for $\Delta\omega\tau_c = 20$, and the RHP Markovian limit is reached with $\Omega = 1.35$. The average energies for $T = 0.33\omega_0$ (RHP Markovian regime) and $T = 0.10\omega_0$ (RHP non-Markovian regime) are

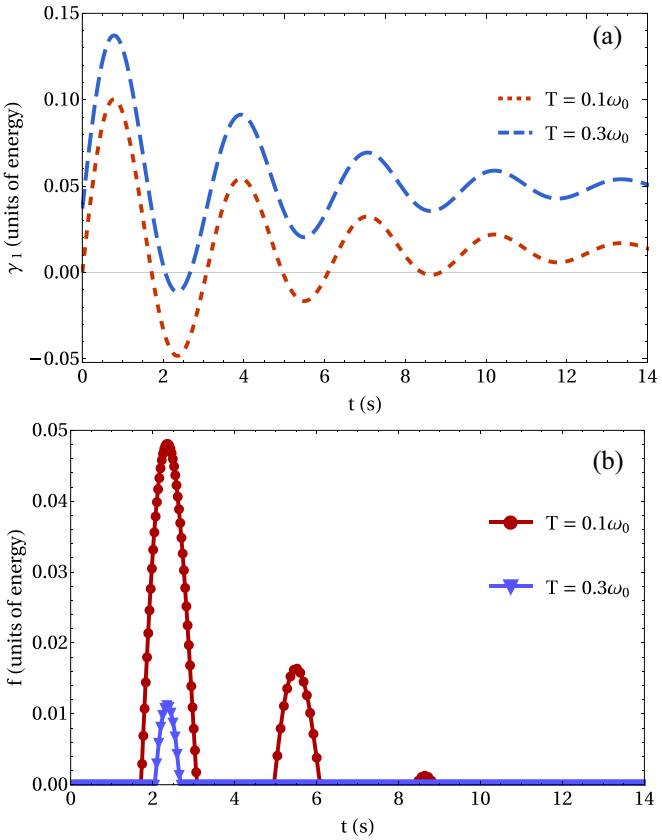

FIG. 3. (a) Decay rate $\gamma_1(t)$, Eq. (55) as a function of time in RHP non-Markovian regime using the exponential pump for two different temperatures, $T = 0.1\omega_0$ (short-dashed red line) and $T = 0.3\omega_0$ (long-dashed blue line) (b) ACHL measure $f(t)$, Eq. (10), as a function of time in the same regime, for the temperatures $T = 0.1\omega_0$ (red solid line with circles) and $T = 0.3\omega_0$ (blue solid line with triangles). The value obtained for the measure were $\mathcal{N}_{\text{ACHL}} = 0.0546$ for $T = 0.1\omega_0$ and $\mathcal{N}_{\text{ACHL}} = 0.0046$ for $T = 0.3\omega_0$. The parameters used were $\Delta\omega = 2$, $\tau_c = 4.25$, $\Omega = 0.91$, $\gamma = 1$.

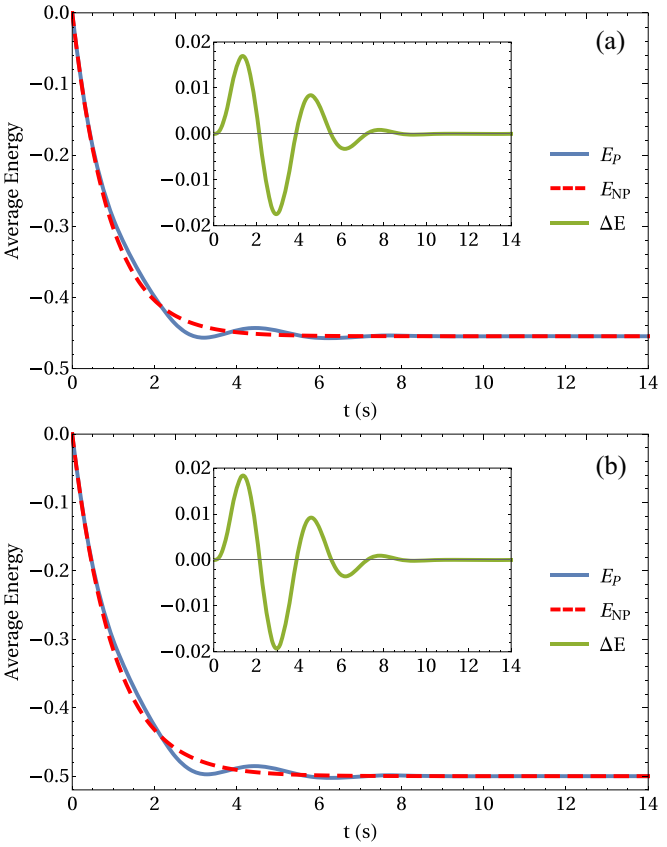

FIG. 4. Average energy of the system with (E_P, blue solid line) and without (E_{NP}, red dashed line) squared exponential pump. Inset shows the average energy difference, defined as $\Delta E = E_P - E_{NP}$. (a) RHP Markovian regime, with $T = 0.33\omega_0$, and (b) RHP non-Markovian regime, with $T = 0.10\omega_0$. The parameters used were $\Delta\omega = 2$, $\tau_c = 4.25$, $\Omega = 0.47$, $\gamma = 1$. We can observe again that the energy differences in the two regimes are equivalent.

plotted in Fig. 6. The short-time limit is

$$\eta_{\text{PL}}(t) \simeq \frac{2\Omega t}{\tau_c}. \tag{76}$$

For $t \to \infty$, we were not able to find an analytical expression, but the decay rate $\gamma_1(t)$ and the ACHL measure $f(t)$ are plotted in Fig. 7(b). The value obtained for the measure were $\mathcal{N}_{\text{ACHL}}$ is 0.0532 for $T = 0.1\omega_0$ and $\mathcal{N}_{\text{ACHL}}$ is 0.0058 for $T = 0.3\omega_0$.

D. Comparisons

The decay rates $\gamma_1(t)$ for the three pumps are plotted in Fig. 8(a) and the average energies in Fig. 8(b) for the RHP non-Markovian case ($T = 0.1\omega_0$). The function $f(t)$, Eq. (10), for the three studied noises, with the parameters as in previous sections and for the case $T = 0.1\omega_0$, is shown in Fig. 9(a), where the blue, yellow, and green lines correspond, respectively, to the exponential, the squared exponential, and the power-law noises. Note that the ACHL measure, Eq. (11), corresponds to the area under the functions, and its numerical values are given in Table I. Since it is clearly positive, the RHP non-Markovianity of the evolution is verified. The values of the measure are approximately $\mathcal{N}^{\text{OU}}_{\text{ACHL}} = 0.0546$, $\mathcal{N}^{\text{SE}}_{\text{ACHL}} = 0.0585$, and $\mathcal{N}^{\text{PL}}_{\text{ACHL}} = 0.0532$ for the exponential, squared exponential, and power-law noises, respectively. In that regime, the three noises are very similar.

For a better comparison among the RHP non-Markovianity generated by the noises, we plotted in Fig. 9(b) the ACHL measure using the parameters of the power-law case, where we find RHP non-Markovianity for all the three cases, and the numerical values for the ACHL measure are in Table I. It can be seen that, for the same parameters, the squared

TABLE I. Numerical value of the ACHL measure for the three noises. The parameters for the second column were $\Delta\omega = 2$, $\tau_c = 4.25$, $\Omega = 0.91$ (OU); $\Delta\omega = 2$, $\tau_c = 4.25$, $\Omega = 0.47$ (SE); $\Delta\omega = 2$, $\tau_c = 10$, $\Omega = 1.35$ (PL). The parameters for the third column were $\Delta\omega = 2$, $\tau_c = 10$, $\Omega = 1.35$. In both cases, we used $\gamma = 1$, $T = 0.1\omega_0$.

Noise	ACHL measure (different parameters)	ACHL measure (same parameters)
Exponential (OU)	0.0546	0.1047
Squared exponential (SE)	0.0585	0.1651
Power law (PL)	0.0532	0.0532

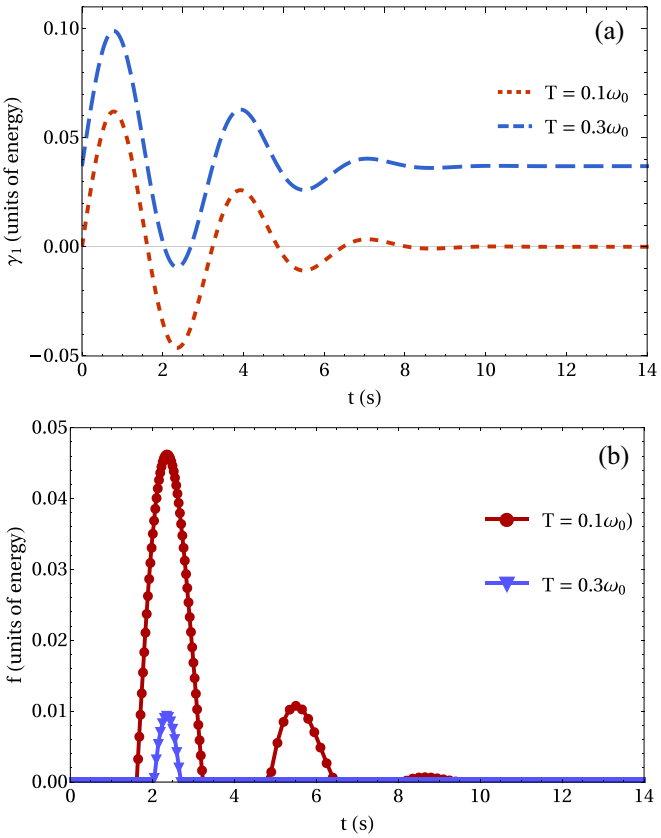

FIG. 5. (a) Decay rate $\gamma_1(t)$, Eq. (55), as a function of time in RHP non-Markovian regime using the square exponential pump for two different temperatures: $T = 0.1\omega_0$ (short-dashed red line) and $T = 0.3\omega_0$ (long-dashed blue line). (b) ACHL measure $f(t)$, Eq. (10), as a function of time in the same regime, for the temperatures $T = 0.1\omega_0$ (red solid line with circles) and $T = 0.3\omega_0$ (blue solid line with triangles). The value obtained for the measure were $\mathcal{N}_{\text{ACHL}} = 0.0585$ for $T = 0.1\omega_0$ and $\mathcal{N}_{\text{ACHL}} = 0.0040$ for $T = 0.3\omega_0$. The parameters used were $\Delta\omega = 2$, $\tau_c = 4.25$, $\Omega = 0.47$, $\gamma = 1$.

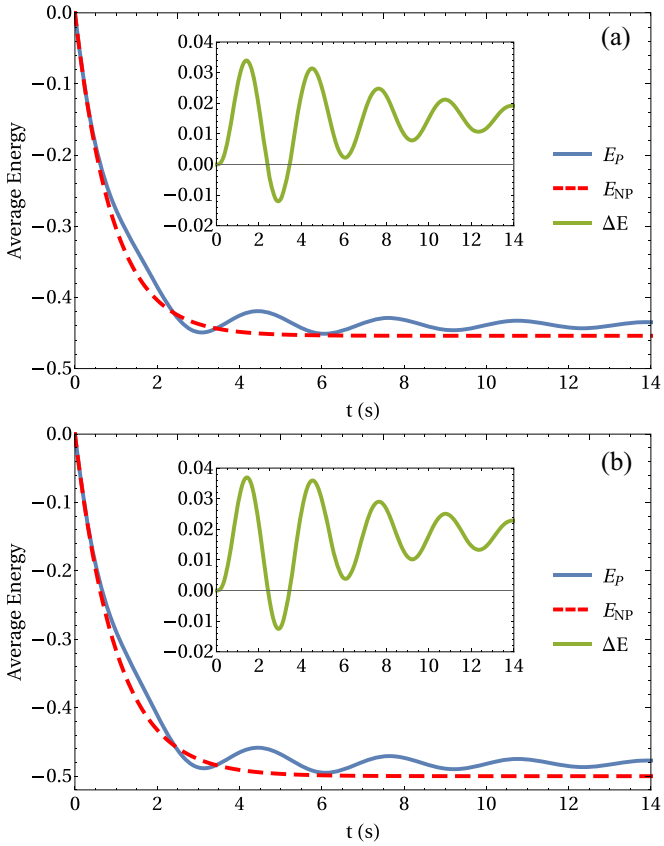

FIG. 6. Average energy of the system with (E_P, blue solid line) and without (E_{NP}, red dashed line) power-law pump. Inset shows the average energy difference, $\Delta E = E_P - E_{NP}$, in (a) RHP Markovian regime, with $T = 0.33\omega_0$, and (b) RHP non-Markovian regime, with $T = 0.10\omega_0$. The parameters used were $\Delta\omega = 2$, $\tau_c = 10$, $\Omega = 1.35$, $\gamma = 1$. We can observe also in this case that the energy differences in the two regimes are equivalent.

exponential noise shows a bigger value in the ACHL measure than the others. Namely, the values are $\mathcal{N}^{\text{OU}}_{\text{ACHL}} = 0.1047$, $\mathcal{N}^{\text{SE}}_{\text{ACHL}} = 0.1651$, and $\mathcal{N}^{\text{PL}}_{\text{ACHL}} = 0.0532$ for the exponential, squared exponential, and power-law noises, respectively. In all these cases, however, the other decay rate $\gamma_2(t)$ is always positive, since the noise strength cannot be large enough to overcome the temperature term $\gamma[N(\omega) + 1)]$, as we are in the weak-coupling regime. Moreover, the sum of the decay rates is always positive as well, since the magnitude of the positive rate results much larger than the magnitude of the negative rate. Therefore, although our evolution is non-Markovian in the RHP sense, it is Markovian by the BLP definition, since the BLP measure (negativity of the sum of the decay rates) is zero.

V. EXPERIMENTAL PROPOSAL

Single trapped ions are a great test bench for reservoir engineering. Changes in the trapping potential and laser-ion interactions can be used to create amplitude and phase reservoirs [85–87]. Another important feature of this system is the ability to do full quantum state tomography [88,89], which is a key feature to see the signature of non-Markovian dynamics in the different types of measurements. Therefore, they are a good candidate to test our proposal.

A linear Paul trap combines oscillating and static electric fields to create an effective static three-dimensional (3D) harmonic potential. If we considered the radial trapping frequency (ω_r) much higher than the axial one (ω) the ion motion is simplified. In this approximation, the net system comprises of one ion in a one-dimensional (1D) harmonic motion. Choosing two internal metastable electronic levels, the ion internal structure can be approximated by a two-level system, which can be represented in the spin 1/2 basis $|\uparrow\rangle$ $|\downarrow\rangle$.

The Hamiltonian that describes the quantum dynamics of the single trapped ion interacting with the light field is

$$H = \frac{\omega_0}{2}\sigma_z + \omega a^\dagger a + \frac{\Omega}{2}(\sigma_+ + \sigma_-) \times [e^{i(kz-\omega_l+\phi)} + e^{-i(kz-\omega_l+\phi)}], \tag{77}$$

where Ω is the coupling strength of the laser, k is the wave number, and ω_l and ϕ are the laser frequency and phase, respectively. There are several approximations and considerations that we can take into account [88] that simplify the Hamiltonian and enable us to express it in terms of the

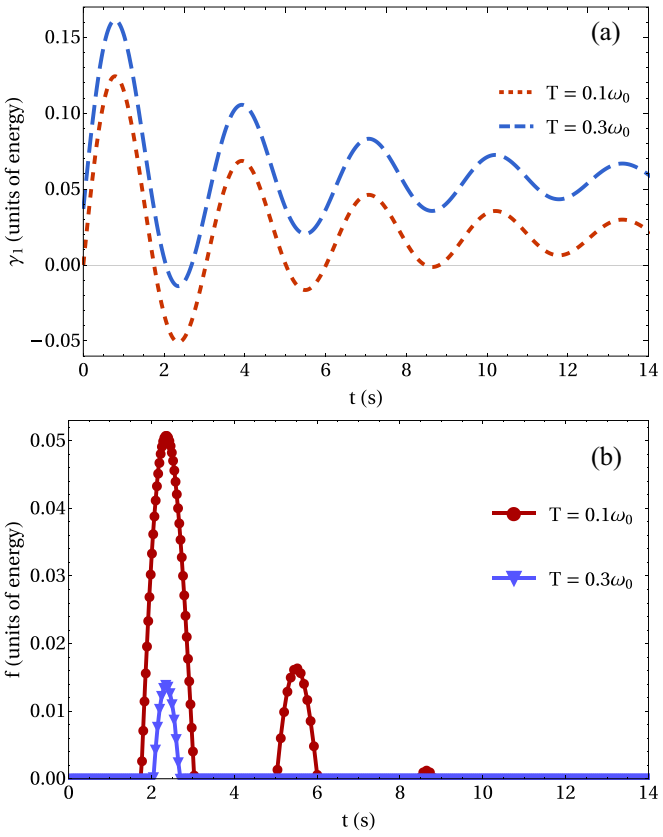

FIG. 7. (a) Decay rate $\gamma_1(t)$, Eq. (55), as a function of time in RHP non-Markovian regime using the power-law pump for two different temperatures: $T = 0.1\omega_0$ (short-dashed red line) and $T = 0.3\omega_0$ (long-dashed blue line) (b) ACHL measure $f(t)$, Eq. (10), as a function of time in the same regime, for the temperatures $T = 0.1\omega_0$ (red solid line with circles) and $T = 0.3\omega_0$ (blue solid line with triangles). The value obtained for the measure were $\mathcal{N}_{\mathrm{ACHL}} = 0.0532$ for $T = 0.1\omega_0$ and $\mathcal{N}_{\mathrm{ACHL}} = 0.0058$ for $T = 0.3\omega_0$. The parameters used were $\Delta\omega = 2$, $\tau_c = 10$, $\Omega = 1.35$, $\gamma = 1$.

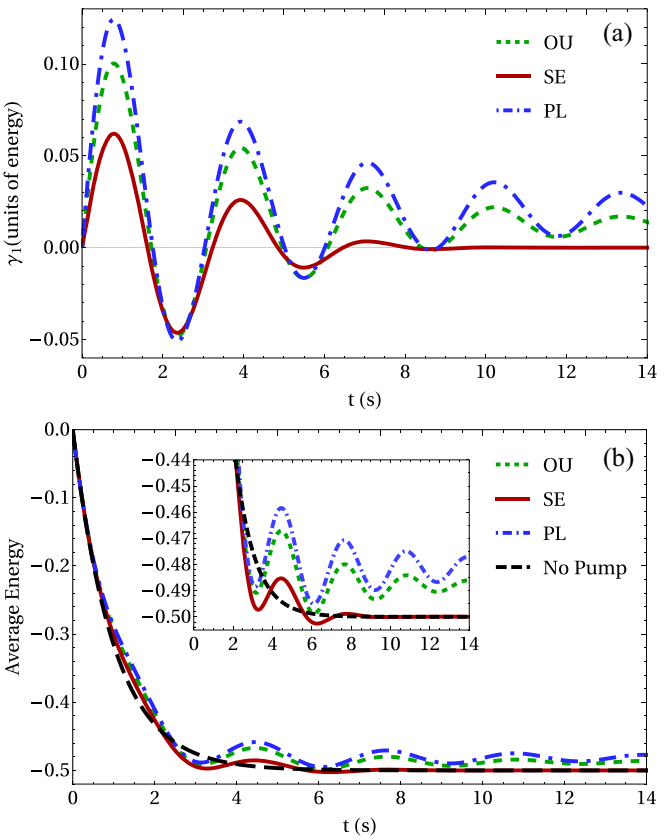

FIG. 8. (a) Decay rate $\gamma_1(t)$, Eq. (55), as a function of time in RHP non-Markovian regime for different noises. The parameters used were $\Delta\omega = 2$, $\tau_c = 4.25$, $\Omega = 0.91$ (OU, green dashed line); $\Delta\omega = 2$, $\tau_c = 4.25$, $\Omega = 0.47$ (SE, red solid line); $\Delta\omega = 2$, $\tau_c = 10$, $\Omega = 1.35$ (PL, dot-dashed blue line). (b) Average energy for different noises. The parameters used were $\Delta\omega = 2$, $\tau_c = 4.25$, $\Omega = 0.91$ (OU, short-dashed green line); $\Delta\omega = 2$, $\tau_c = 4.25$, $\Omega = 0.47$ (SE, red solid line); $\Delta\omega = 2$, $\tau_c = 10$, $\Omega = 1.35$ (PL, dot-dashed blue line); average energy of the system without pump (long-dashed black line). Inset shows a comparison of average energies on a better scale. All the curves used have $\gamma = 1$, $T = 0.1\omega_0$.

harmonic-oscillator operators of creation and annihilation:

$$H = \frac{\omega_0}{2}\sigma_z + \omega a^\dagger a + \frac{\Omega}{2}[e^{i\eta(a+a^\dagger)}\sigma_+ e^{-i(\omega_l+\phi)} + e^{-i\eta(a+a^\dagger)}\sigma_- e^{+i(\omega_l+\phi)}], \tag{78}$$

where the Lamb–Dicke parameter is defined as

$$\eta = k\sqrt{\frac{\hbar}{2m_0\omega}}. \tag{79}$$

With laser cooling methods the ion motion can be prepared near to the ground state of the oscillator [88]. This is known as the Lamb–Dicke regime, where $\eta \ll 1$. Therefore, we can consider that the average vibrational occupation number is negligible. In this regime the exponential terms can be expanded in powers of η. Keeping only the terms up to first order η the light-field–ion interaction is described by three resonant terms:

$$H_{\mathrm{c}} = \tfrac{1}{2}\hbar\Omega_c n(\sigma_+ e^{-i\phi} + \sigma_- e^{i\phi}), \tag{80}$$

$$H_{\mathrm{rsb}} = \tfrac{1}{2}\hbar\Omega_{\mathrm{sb}}(a\sigma_+ e^{-i\phi} - a^\dagger\sigma_- e^{i\phi}), \tag{81}$$

$$H_{\mathrm{bsb}} = \tfrac{1}{2}\hbar\Omega_{\mathrm{sb}}(a^\dagger\sigma_+ e^{-i\phi} - a\sigma_- e^{i\phi}), \tag{82}$$

where $\Omega_c = \Omega(1-\eta^2)$, $\Omega_{\mathrm{sb}} = \eta\Omega$ are the coupling strength of the Raman transitions. The first term is the Carrier transition; this coupling changes only the internal degree of freedom, the ion motion is kept intact. The second (third) term couples the internal degree of freedom with the motion. It connects the states $|\downarrow,n\rangle \leftrightarrow |\uparrow,n-1\rangle$ ($|\downarrow,n\rangle \leftrightarrow |\uparrow,n+1\rangle$). Therefore, it is known as the red-side band (blue-side band) transition.

We can see that the two-level system coupled to a harmonic bath plus colored noise can be fully simulated by a combination of these transitions. In fact, comparing the terms above with the interaction term of the Hamiltonian of Eq. (29), for a suitable choice of the laser phase, the red-side band interaction mimics the amplitude damping Hamiltonian, where the environment has only one mode of vibration. The noise is

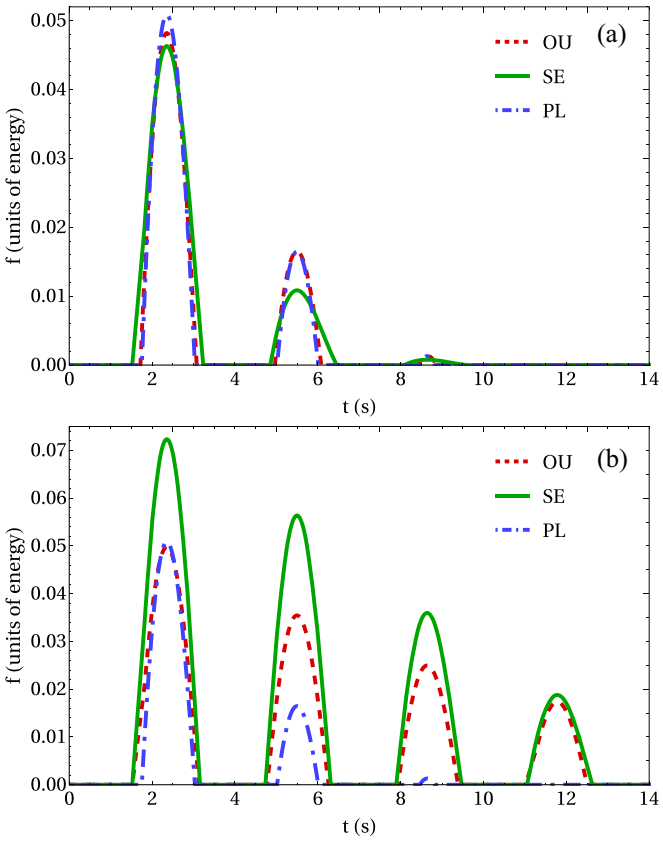

FIG. 9. ACHL measure $f(t)$ for different noises. (a) The parameters used were $\Delta\omega = 2$, $\tau_c = 4.25$, $\Omega = 0.91$ (OU, red dashed line); $\Delta\omega = 2$, $\tau_c = 4.25$, $\Omega = 0.47$ (SE, green solid line); $\Delta\omega = 2$, $\tau_c = 10$, $\Omega = 1.35$ (PL, dot-dashed blue line). (b) The parameters used were $\Delta\omega = 2$, $\tau_c = 10$, $\Omega = 1.35$. All curves used $\gamma = 1$, $T = 0.1\omega_0$.

modeled by using a stochastic time-dependent light field in the Carrier transition. Experimentally this can be achieved with an arbitrary function generator and an acousto-optic modulator to adjust the amplitude and phase of the laser. The Markovian temperature, in this case, will be related to the ratio between the blue-side band and the Carrier laser intensities.

We can go one step further and couple one oscillator system to a oscillator bath, as was done by Myatt *et al.*[86]. They used the superposition of coherent motion states to study decoherence through the coupling to engineered amplitude and phase reservoirs. In the experiment, the amplitude reservoir was created by adding a white noise in the trap electric field and the phase damping by modulating the trap frequency with that noise. Using this technique they were able to engineer high-temperature and zero-temperature reservoirs. The system was prepared in a superposition of coherent motion states and its coherence as function of the size of the superposition was measured with single-atom interferometry [86]. Adding a colored noise to the white noise, the non-Markovian dynamics could be seen as a revival of the interference fringes.

VI. CONCLUSIONS AND OUTLOOK

We have investigated the dynamics of a system subjected to a classical colored noise and shown that this pump indeed induces quantum non-Markovianity. We have considered a qubit interacting with a bosonic environment and undergoing a Markovian evolution. After turning on the classical noise, the evolution becomes non-Markovian, as witnessed by the ACHL measure applied to the master equation of the system. We have analyzed three different colored noises, showing that the squared exponential noise is the more efficient one to produce this effect.

The evolution of the system has been decomposed in two parts: system-bath and system-pump evolutions. In the first the qubit exchanges energy with a bosonic bath, and a Markovian master equation has been derived under the Born–Markov setting [1,2]. For the second, the noise has been modelled by a stochastic Hamiltonian and functional calculus and, together with a weak-coupling assumption, has been used in order to derive a master equation [64]. In this case, we have found that the evolution can become non-Markovian, depending on the noise parameters. Having the master equation, we have been able to evaluate the RHP non-Markovianity of the system evolution by analysis of its decay rates, according to the ACHL measure [75].

Three noises have been used in the subsequent analysis: exponential (Ornstein–Uhlenbeck), squared exponential, and power-law noises [67]. The idea has been to subject the system to an environment at $T = 0.33\omega_0$ and find the minimum values of the parameters of each noise required to reach the RHP Markovianity limit. Physically we have been interested in the minimum noise strength necessary to overcome the decohering effects of the bath and reverse the energy flow. Cooling the environment to $T = 0.10\omega_0$ with fixed noise parameters, we have been able to measure the RHP non-Markovianity of the system dynamics associated with each noise. The noises have been then compared under the same values of the parameters, with the ACHL measure for the squared exponential noise exhibiting bigger values, which shows that, among the three noises, it can generate more quantum non-Markovianity. The noise pumps also have been found to cause the system's average energy to oscillate and increase from the value they reach without the pump. This increase in value, however, results almost independent of the temperature. Since the energy differences between Markovian and non-Markovian regimes are equivalent to all noise, the energy required to carry from one regime to another is low.

Our results suggest further interesting studies within the context of open quantum systems. For instance, the formalism developed here could be applied to actual quantum systems for investigating to which extent (i) the injection of noise acts as a reliable alternative to reservoir engineering and (ii) the non-Markovian features of the model are relevant to decoherence suppression or preservation of information. Moreover, the model could be exploited for quantum thermal machines [90,91] to verify its possible role in enabling useful thermodynamical features, such as increased efficiencies of cycles.

ACKNOWLEDGMENTS

The authors would like to thank G. Adesso, F. F. Fanchini, and M. H. Y. Moussa for fruitful conversations. The authors would like to acknowledge the financial support from Brazilian funding agencies CNPq (Grants No. 304955/2013-2 and

No. 443828/2014-8), CAPES Pesquisador Visitante Especial (Grant No. 108/2012), FAPESP (Grant No. 2014/09566-0), and the Brazilian National Institute of Science and Technology of Quantum Information (INCT/IQ).

[1] H.-P. Breuer and F. Petruccione, *The Theory of Open Quantum Systems* (Oxford University Press, Oxford, 2007).
[2] A. Rivas and S. F. Huelga, *Open Quantum Systems* (Springer, Berlin, 2012).
[3] H. Carmichael, *An Open Systems Approach to Quantum Optics*, Lecture Notes in Physics (Springer, Berlin, 1993).
[4] R. Alicki and K. Lendi, *Quantum Dynamical Semigroups and Applications* (Springer, Berlin, 2007).
[5] E. Davis, *Quantum Theory of Open Systems* (Academic Press, New York, 1976).
[6] U. Weiss, *Quantum Dissipative Systems*, 4th ed. (World Scientific Publishing Co., Singapore, 2012).
[7] E. Joos, H. D. Zeh, C. Kiefer, D. Giulini, J. Kupsch, and I.-O. Stamatescu, *Decoherence and the Appearance of a Classical World in Quantum Theory* (Springer, Berlin, 2003).
[8] W. H. Zurek, Rev. Mod. Phys. **75**, 715 (2003).
[9] Á. Rivas, S. F. Huelga, and M. B. Plenio, Rep. Prog. Phys. **77**, 094001 (2014).
[10] H.-P. Breuer, E.-M. Laine, J. Piilo, and B. Vacchini, Rev. Mod. Phys. **88**, 021002 (2016).
[11] M. M. Wolf, J. Eisert, T. S. Cubitt, and J. I. Cirac, Phys. Rev. Lett. **101**, 150402 (2008).
[12] J. Piilo, S. Maniscalco, K. Härkönen, and K.-A. Suominen, Phys. Rev. Lett. **100**, 180402 (2008).
[13] I. de Vega and D. Alonso, Rev. Mod. Phys. **89**, 015001 (2017).
[14] F. A. Pollock, C. Rodríguez-Rosario, T. Frauenheim, M. Paternostro, and K. Modi, arXiv:1512.00589.
[15] F. Brito and T. Werlang, New J. Phys. **17**, 072001 (2015).
[16] Á. Rivas, S. F. Huelga, and M. B. Plenio, Phys. Rev. Lett. **105**, 050403 (2010).
[17] B. Bylicka, D. Chruściński, and S. Maniscalco, Sci. Rep. **4**, 5720 (2014).
[18] C. Addis, B. Bylicka, D. Chruściński, and S. Maniscalco, Phys. Rev. A **90**, 052103 (2014).
[19] B. Leggio, R. Lo Franco, D. O. Soares-Pinto, P. Horodecki, and G. Compagno, Phys. Rev. A **92**, 032311 (2015).
[20] S. Lloyd and L. Viola, Phys. Rev. A **65**, 010101 (2001).
[21] A. W. Chin, S. F. Huelga, and M. B. Plenio, Phys. Rev. Lett. **109**, 233601 (2012).
[22] F. Verstraete, M. M. Wolf, and J. I. Cirac, Nat. Phys. **5**, 633 (2009).
[23] Z.-X. Man, Y.-J. Xia, and R. Lo Franco, Sci. Rep. **5**, 13843 (2015).
[24] Z.-X. Man, Y.-J. Xia, and R. Lo Franco, Phys. Rev. A **92**, 012315 (2015).
[25] K. F. Romero and R. Lo Franco, Phys. Scr. **86**, 065004 (2012).
[26] R. Lo Franco, New J. Phys. **17**, 081004 (2015).
[27] R. Lo Franco, Quantum Inf. Process. **15**, 2393 (2016).
[28] C. A. González-Gutiérrez, R. Román-Ancheyta, D. Espitia, and R. Lo Franco, Int. J. Quantum Inform. **14**, 1650031 (2016).
[29] N. van Kampen, *Stochastic Processes in Physics and Chemistry*, 3rd ed. (North-Holland, Amsterdam, 2007).
[30] L. Accardi, in *Statistical Physics and Dynamical Systems*, edited by J. Fritz, A. Jaffe, and D. Szász (Springer, Berlin, 1985), pp. 285–302.
[31] P. Haikka, J. D. Cresser, and S. Maniscalco, Phys. Rev. A **83**, 012112 (2011).
[32] A. C. Neto, G. Karpat, and F. F. Fanchini, Phys. Rev. A **94**, 032105 (2016).
[33] H.-P. Breuer, E.-M. Laine, and J. Piilo, Phys. Rev. Lett. **103**, 210401 (2009).
[34] L. Viola, E. Knill, and S. Lloyd, Phys. Rev. Lett. **82**, 2417 (1999).
[35] G. Guarnieri, C. Uchiyama, and B. Vacchini, Phys. Rev. A **93**, 012118 (2016).
[36] S. Deffner and E. Lutz, Phys. Rev. Lett. **111**, 010402 (2013).
[37] M. Pezzutto, M. Paternostro, and Y. Omar, New J. Phys. **18**, 123018 (2016).
[38] S. F. Huelga, Á. Rivas, and M. B. Plenio, Phys. Rev. Lett. **108**, 160402 (2012).
[39] R. Lo Franco, B. Bellomo, S. Maniscalco, and G. Compagno, Int. J. Mod. Phys. B **27**, 1345053 (2013).
[40] B. Bellomo, R. Lo Franco, and G. Compagno, Phys. Rev. Lett. **99**, 160502 (2007).
[41] R. Lo Franco, A. D'Arrigo, G. Falci, G. Compagno, and E. Paladino, Phys. Rev. B **90**, 054304 (2014).
[42] A. D'Arrigo, R. Lo Franco, G. Benenti, E. Paladino, and G. Falci, Ann. Phys. (NY) **350**, 211 (2014).
[43] L. Aolita, F. de Melo, and L. Davidovich, Rep. Prog. Phys. **78**, 042001 (2015).
[44] A. Mortezapour, M. A. Borji, and R. Lo Franco, Laser Phys. Lett. **14**, 055201 (2017).
[45] R. Lo Franco, B. Bellomo, E. Andersson, and G. Compagno, Phys. Rev. A **85**, 032318 (2012).
[46] F. Galve, R. Zambrini, and S. Maniscalco, Sci. Rep. **6**, 19607 (2016).
[47] B.-H. Liu, X.-M. Hu, Y.-F. Huang, C.-F. Li, G.-C. Guo, A. Karlsson, E.-M. Laine, S. Maniscalco, C. Macchiavello, and J. Piilo, Europhys. Lett. **114**, 10005 (2016).
[48] R. Vasile, S. Olivares, M. G. A. Paris, and S. Maniscalco, Phys. Rev. A **83**, 042321 (2011).
[49] R. Schmidt, A. Negretti, J. Ankerhold, T. Calarco, and J. T. Stockburger, Phys. Rev. Lett. **107**, 130404 (2011).
[50] N. K. Bernardes, J. P. S. Peterson, R. S. Sarthour, A. M. Souza, C. H. Monken, I. Roditi, I. S. Oliveira, and M. F. Santos, Sci. Rep. **6**, 33945 (2016).
[51] A. Souza, J. Li, D. Soares-Pinto, R. Sarthour, I. S. Oliveira, S. Huelga, M. Paternostro, and F. Semião, arXiv:1308.5761.
[52] A. Orieux, A. DArrigo, G. Ferranti, R. Lo Franco, G. Benenti, E. Paladino, G. Falci, F. Sciarrino, and P. Mataloni, Sci. Rep. **5**, 8575 (2015).
[53] B.-H. Liu, L. Li, Y.-F. Huang, C.-F. Li, G.-C. Guo, E.-M. Laine, H.-P. Breuer, and J. Piilo, Nat. Phys. **7**, 931 (2011).
[54] F. F. Fanchini, G. Karpat, B. Çakmak, L. K. Castelano, G. H. Aguilar, O. J. Farías, S. P. Walborn, P. H. Souto Ribeiro, and M. C. de Oliveira, Phys. Rev. Lett. **112**, 210402 (2014).

[55] J.-S. Xu, K. Sun, C.-F. Li, X.-Y. Xu, G.-C. Guo, E. Andersson, R. Lo Franco, and G. Compagno, Nat. Commun. **4**, 2851 (2013).
[56] H.-N. Xiong, W.-M. Zhang, X. Wang, and M.-H. Wu, Phys. Rev. A **82**, 012105 (2010).
[57] T. B. Batalhão, G. D. de Moraes Neto, M. A. de Ponte, and M. H. Y. Moussa, Phys. Rev. A **90**, 032105 (2014).
[58] H. Krovi, O. Oreshkov, M. Ryazanov, and D. A. Lidar, Phys. Rev. A **76**, 052117 (2007).
[59] A. W. Chin, J. Prior, R. Rosenbach, F. Caycedo-Soler, S. F. Huelga, and M. B. Plenio, Nat. Phys. **9**, 113 (2013).
[60] P. C. Cárdenas, M. Paternostro, and F. L. Semião, Phys. Rev. A **91**, 022122 (2015).
[61] H.-B. Chen, N. Lambert, Y.-C. Cheng, Y.-N. Chen, and F. Nori, Sci. Rep. **5**, 12753 (2015).
[62] A. A. Budini, A. K. Chattah, and M. O. Cáceres, J. Phys. A: Math. Gen. **32**, 631 (1999).
[63] A. A. Budini, Phys. Rev. A **63**, 012106 (2000).
[64] A. A. Budini, Phys. Rev. A **64**, 052110 (2001).
[65] D. F. V. James, Phys. Rev. Lett. **81**, 317 (1998).
[66] C. Benedetti, F. Buscemi, P. Bordone, and M. G. A. Paris, Phys. Rev. A **87**, 052328 (2013).
[67] C. Benedetti and M. G. Paris, Phys. Lett. A **378**, 2495 (2014).
[68] R. Lo Franco and G. Compagno, arXiv:1608.05970.
[69] A. Chenu, M. Beau, J. Cao, and A. del Campo, Phys. Rev. Lett. **118**, 140403 (2017).
[70] M. B. Plenio and P. L. Knight, Rev. Mod. Phys. **70**, 101 (1998).
[71] J. Dalibard, Y. Castin, and K. Mølmer, Phys. Rev. Lett. **68**, 580 (1992).
[72] E. A. Novikov, Sov. Phys. JETP **20**, 1290 (1965).
[73] F. Moss and P. McClintock, *Noise in Nonlinear Dynamical Systems: Volume 1, Theory of Continuous Fokker-Planck Systems* (Cambridge University Press, Cambridge, 1989).
[74] V. S. Vladimirov, *Methods of the Theory of Generalized Functions (Analytical Methods and Special Functions)*, 1st ed. (CRC Press, Boca Raton, Florida, 2002).
[75] M. J. W. Hall, J. D. Cresser, L. Li, and E. Andersson, Phys. Rev. A **89**, 042120 (2014).
[76] D. Chruściński and S. Maniscalco, Phys. Rev. Lett. **112**, 120404 (2014).
[77] G. Lindblad, Commun. Math. Phys. **48**, 119 (1976).
[78] M.-D. Choi, Lin. Alg. Appl. **10**, 285 (1975).
[79] A. Jamiołkowski, Rep. Math. Phys. **3**, 275 (1972).
[80] M. A. Nielsen and I. L. Chuang, *Quantum Computation and Quantum Information: 10th Anniversary Edition* (Cambridge University Press, Cambridge, 2012).
[81] S. Lorenzo, F. Plastina, and M. Paternostro, Phys. Rev. A **88**, 020102 (2013).
[82] L. E. Ballentine, *Quantum Mechanics: A Modern Development*, 2nd ed. (World Scientific Publishing Co., Singapore, 1998).
[83] D. A. Lidar, Z. Bihary, and K. Whaley, Chem. Phys. **268**, 35 (2001).
[84] M. Moussa, S. Mizrahi, and A. Caldeira, Phys. Lett. A **221**, 145 (1996).
[85] J. F. Poyatos, J. I. Cirac, and P. Zoller, Phys. Rev. Lett. **77**, 4728 (1996).
[86] Q. A. Turchette, C. J. Myatt, B. E. King, C. A. Sackett, D. Kielpinski, W. M. Itano, C. Monroe, and D. J. Wineland, Phys. Rev. A **62**, 053807 (2000).
[87] D. Kienzler, H.-Y. Lo, B. Keitch, L. de Clercq, F. Leupold, F. Lindenfelser, M. Marinelli, V. Negnevitsky, and J. P. Home, Science **347**, 53 (2015).
[88] D. Leibfried, R. Blatt, C. Monroe, and D. Wineland, Rev. Mod. Phys. **75**, 281 (2003).
[89] C. F. Roos, G. P. T. Lancaster, M. Riebe, H. Häffner, W. Hänsel, S. Gulde, C. Becher, J. Eschner, F. Schmidt-Kaler, and R. Blatt, Phys. Rev. Lett. **92**, 220402 (2004).
[90] J. P. Palao, R. Kosloff, and J. M. Gordon, Phys. Rev. E **64**, 056130 (2001).
[91] Y. Rezek, P. Salamon, K. H. Hoffmann, and R. Kosloff, Europhys. Lett. **85**, 30008 (2009).